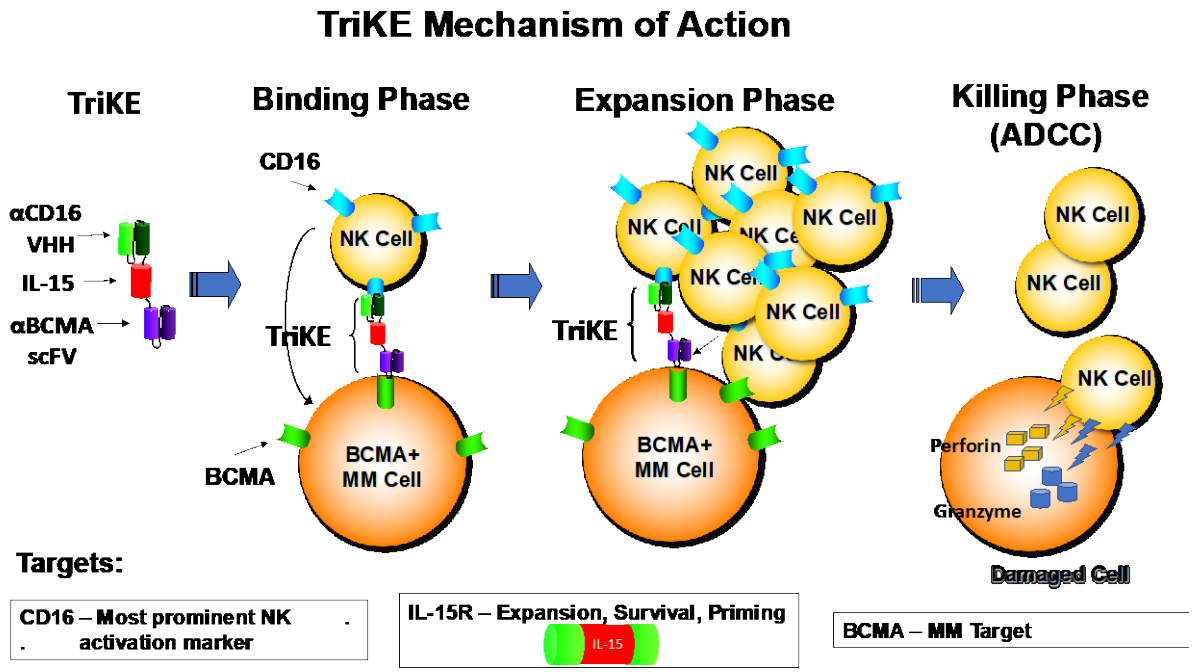

Figure S1. TriKe Mechanism of Action. Trike mechanism can be sorted into discrete steps controlled by IL-15 activation signals. 1) In the binding phase, the anti-CD16 moiety of 1615BCMA binds to NK cells and the anti-BCMA moiety binds to MM cells. The anti-CD16 provides an activation signal that readies NK cells for the killing process. 2) In the expansion phase, the IL-15 moiety binds to IL-15R expressed on NK cells triggering further NK cells proliferation at the cancer site. More NK cells join the frenzy. The cytotoxic process in NK cells is influenced by IL-15 activation signals. 3) In the killing phase, cancer cell recognition, facilitated by the drug results in NK cells now gathering perforin- and granzyme-containing cytolytic granules around the microtubule organizing center that focuses the structure on a cancer cell contact point known as the immune synapse. The granules are released onto the cancer cell where the perforin tears holes in the tumor membrane. These pores allow granzymes to enter and induce caspase-dependent cell death. Since IL-15 alone does not facilitate tumor killing in this manner, this indicates that antibody dependent cell mediated toxicity (ADCC) mediated by the anti-CD16 and anti-BCMA binding and not the IL-15 are critical in this phase of killing. .

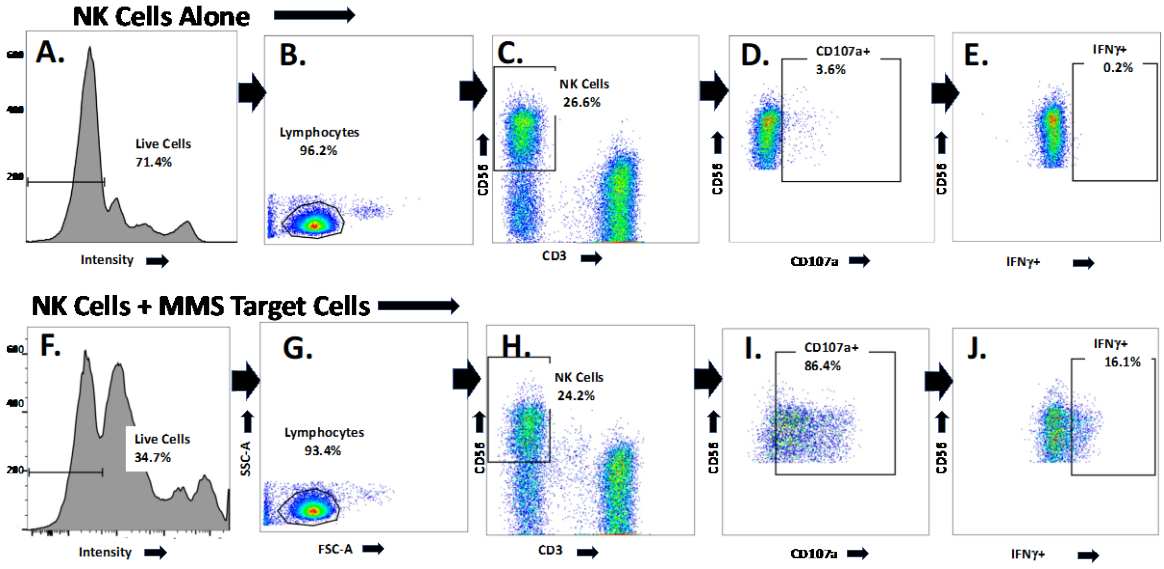

Figure S2. Representative gating strategy for determining levels of CD107a appearing at the cell surface and accumulation of intracellular cytokine IFNγ. The figure explains in greater detail the gating strategy used to quantitate both CD107a expressing NK cells and measure accumulation of

intracellular cytokine IFNγ in PBMC. Panels A – E (upper panels) show the strategy for studies of NK cells without the addition of MM.1S targets while panels F – J show strategy for NK cells in the presence of MMS targets. First, viable cells were gated with the Live/Dead Aqua Staining Kit (Cat. No: L-34966, Thermo Fisher) (Panel A). Next, forward/side gating allowed for gating the predominant population (96.2%) of lymphocytes (Panel B). NK cells were gated using a combination of anti-CD56-PE-Cy7 and anti-CD3-PE-CF594 resulting in an expected 26.6% yield (Panel C). In panel D, cells were stained with FITC-conjugated anti-CD107a (H4A3, BioLegend) to determine the level of cells expressing cell surface CD107a. In Panel E, cells were fixed in 2% paraformaldehyde (Fisher Scientific cat#: 50980487) and permeabilized (eBioscience cat#: 00–8333–56). Permeabilized cells were stained with BV650-conjugated IFNγ (4S.B3, BioLegend), and were evaluated. Cells were run on an LSRII flow cytometer and analyzed using FlowJo software (BD Biosciences). Panels F – J show the identical strategy for NK cells in the presence of MM.1S targets cells and allow for a direct comparison to panels A – E. .

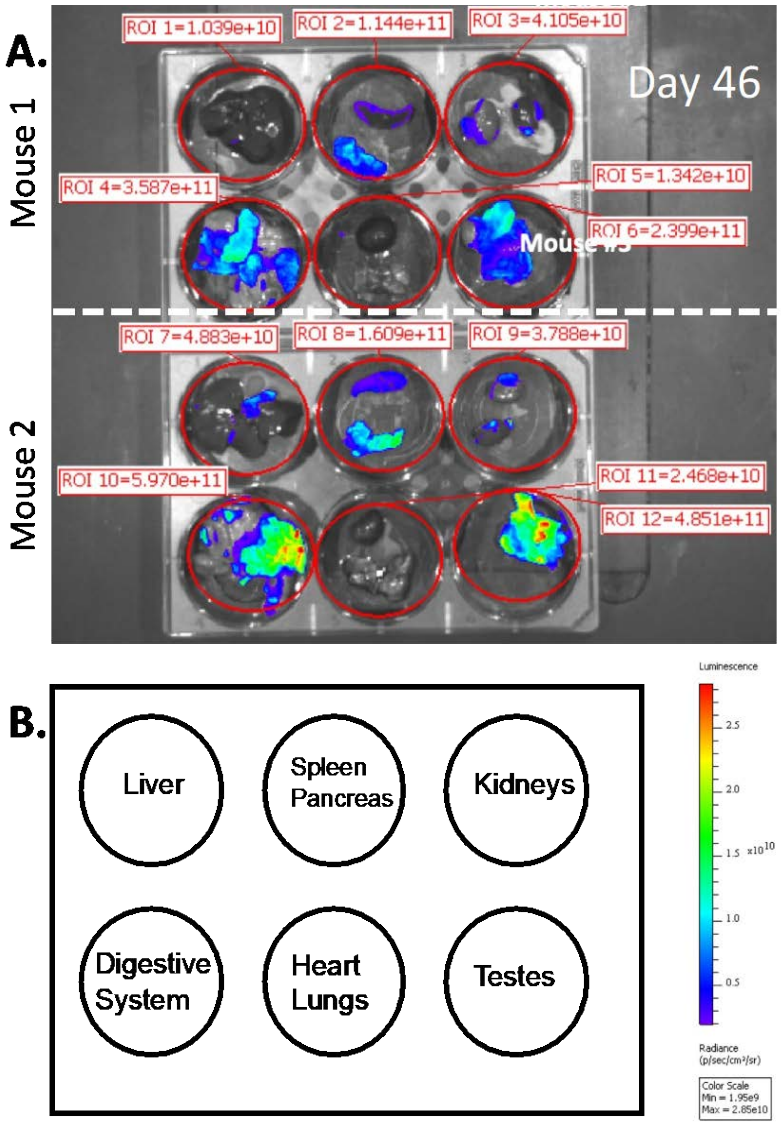

Figure S3. MM.1S tumor progression is aggressive in vivo. To determine the metastatic ability of MM.1S multiple myeloma, two NSG mice that had been injected with 7.5 x 10^5 MM.1S-luc cells were organ imaged. Forty-six days after injection with MM.1S-luc cells, organs were harvested from both mice and imaged for tumor bioluminescence. (A) Tumor progression in the liver (top left), spleen and pancreas (top middle), kidneys (top right), digestive system (bottom left), heart and lungs (bottom middle), and testes (bottom right) on day 46 from mouse 1 (top) and mouse 2 (bottom) are shown on a six-well plate. Bioluminescence is shown as a function of photons/s/cm2/sr. Figure 6B shows the plate set-up.